Pergamon

Cement and Concrete Research, Vol. 28, No. 2, pp. 231–243, 1998

0008-8846/98 $19.00 + .00

PII S00008-8846(97)00260-3

QUASIELASTIC NEUTRON SCATTERING STUDY OF THE EFFECT OF WATER-TO-CEMENT RATIO ON THE HYDRATION KINETICS OF TRICALCIUM SILICATE

R. Berliner,[1]* M. Popovici,* K.W. Herwig,* M. Berliner,* H.M. Jennings,† and J.J. Thomas†

*Research Reactor Center, University of Missouri, Columbia, MO 65211

†Department of Materials Science, Northwestern University, Evanston, IL 60208

(Received May 21, 1997; in final form November 17, 1997)

ABSTRACT

Quasielastic neutron scattering (QNS) measurements of the hydration kinetics of tricalcium silicate (C_3S) have been made with 60 μeV energy resolution at a momentum transfer $q = 1$ Å^{-1}. Monitoring the fraction of neutrons elastically scattered from C_3S paste specimens follows the progress of the C_3S hydration reactions. Three different water/cement ratios (w/c = 0.3, 0.5, and 0.7) were studied in this experiment. Analysis of the rate of reaction over the first approximately 15 h was by an Avrami model. After this time, the rate of hydration no longer follows nucleation and growth kinetics but enters a diffusion controlled regime. At this point, the rate of hydration depends strongly on the w/c, with more reaction at higher w/c ratios. A shrinking core model was used to analyze the diffusion-limited portion of the reaction at later times. The values of the apparent diffusion constant obtained from these data indicate a log-linear relationship between the diffusion constants and the w/c ratio. © *1998 Elsevier Science Ltd*

Introduction

When ordinary Portland cement (OPC) is mixed with water, a period of rapid reaction lasting only a few minutes is followed by an induction period during which the hydration reactions proceed at a much slower rate. After a period of a few hours, the rate of reaction increases again and the cement begins to harden. Many investigators have studied the process of cement hydration with a variety of tools because understanding of and control over the cement hardening process is obviously of great economic importance. These efforts have been summarized in the recent comprehensive work by Taylor (1). Nevertheless, many details of the cement hydration process remain controversial because of inherent difficulties posed by the cement system.

Ordinary Portland cement is a heterogeneous material. Composed of four major and several minor crystalline compounds, the phase composition of an OPC can be highly

[1]To whom correspondence should be addressed.

variable. In addition, the structure and reactivity of the individual compounds themselves are strongly influenced by the conditions under which they are formed and stored, the type and concentration of impurities, the nature and concentration of their structural disorder, and their particle size distribution. Some simplification of the cement hydration problem can be obtained by studying the individual cement compounds instead of OPC.

The rate of hydration of cement compounds such as C_3S is normally measured by thermal calorimetry, which gives the overall kinetics at early times but does not measure the rate of product formation directly. Quantitative x-ray diffraction analysis (QXDA) can be used to measure the rate at which the starting compound is consumed, and ignition techniques can be employed to measure the amount of chemically bound water, but neither of these techniques can be used to monitor the early kinetics. It is very difficult to directly measure the rate of product formation at early times because the main reaction product of C_3S and of Portland cement, the C-S-H gel, is amorphous and is therefore not amenable to diffraction analysis.

The inherent difficulties of characterizing the products and the rate of the hydration reactions has encouraged the development of new analytical tools. Recently, real-time measurements of the progress of cement hydration using neutron diffraction (2), Raman scattering (3), and synchrotron x-ray diffraction (4) have been reported. In addition, Livingston and co-workers (5,6,7) have shown that quasielastic neutron scattering can be used to probe the chemical state of water in the cement system. With QNS, the rate of reaction product formation can be measured by determining the rate at which freely diffusing pore water is converted into bound water within the reaction product.

Neutrons incident on a hydrating cement paste are observed to scatter both elastically and inelastically. These observations are dominated by the scattering from hydrogen because of its large incoherent scattering cross section compared to other elements present in a cement paste (8). Theoretical analysis (9) of the intensity and energy distribution of the scattered neutrons shows that the elastically scattered component has a Gaussian distribution in energy of a width determined by the energy resolution of the instrument. The integrated intensity of this component is directly proportional to the number of hydrogen nuclei that are chemically bound to the cement gel and hence immobile. The inelastically scattered neutrons exhibit a Lorentzian energy distribution with a width that is related to the state of diffusion (translational and rotational) of the hydrogen atoms over a time scale given by $\delta t \sim h/(2\pi\ \delta E)$ and a distance scale given by $\delta x \sim 2\pi/q$. Here, h is Plank's constant, λ is the neutron wavelength, and δE is the energy resolution of the instrument at neutron momentum transfer $q = (4\pi/\lambda)$ sin θ at a neutron scattering angle of 2θ (9). Because the cement paste, pore water, and hydration products contain hydrogen atoms, these characteristics make quasielastic neutron scattering ideal for the study of the rate of reaction in hydrating cements.

Quasielastic neutron scattering measurements of a hydrating cement paste can directly quantify the fraction of water in the specimen that is chemically bound. If the stoichiometry of the reaction is sufficiently well understood, the bound water index (ratio of chemically bound water to total water) can be converted to the degree of reaction and the measurements used for detailed studies of the reaction kinetics. We found it necessary to use a series of specimens to obtain the complete time sequence. Although reproducibility of the results for specimens prepared at different times was generally good, there are some data points that deviate significantly from the norm. We attribute these deviations to mispositioning the sample in the neutron beam (10).

We report here the analysis of the hydration kinetics of tricalcium silicate using quasielastic neutron scattering. The use of tricalcium silicate instead of ordinary Portland cement was

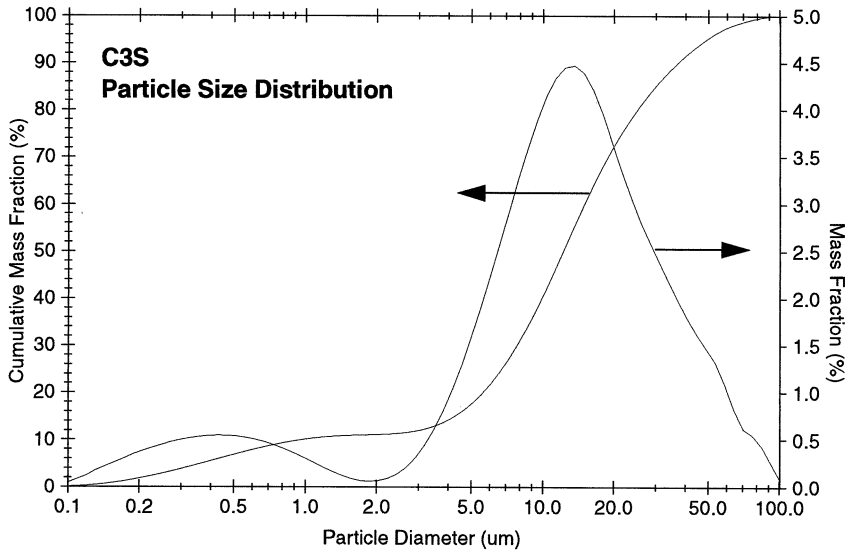

FIG. 1.
Differential and cumulative particle size distribution for the C_3S specimen material as measured by optical interference.

motivated by the desire to avoid the complexity and variability of OPC and to enable us to make detailed comparisons to the studies of this material by other workers.

Experimental

Specimens for this study were made from phase-pure, synthetic, monoclinic tricalcium silicate mixed with de-ionized water at various water-to-cement (w/c) ratios by mass. The structure of the C_3S specimen material was verified using neutron powder diffraction (11). Figure 1 shows the results of a measurement of the C_3S particle size distribution (12). The Blaine fineness specification for the C_3S used in this experiment is 3602 cm^2/g. It is evident that the grain radius obtained using the fineness specification (2.6 μm) is at considerable variance with the measured mean of the distribution (18.2 μm).

The C_3S pastes were prepared in small plastic bags excluding air as much as possible to avoid carbonation from atmospheric CO_2. After the paste had been kneaded to a smooth consistency, usually requiring about 1 min., a corner of the bag was cut away and the paste was extruded into the specimen holder.

The specimen holder consists of a 0.5-mm thick cadmium metal window frame, which is glued with rubber cement to a wafer of semiconductor-grade silicon. After the cement paste was extruded into the center depression, a second silicon wafer was glued to the window frame, creating a sealed silicon-cement-silicon sandwich.

The pore water in a cement paste is strongly basic, usually reaching a condition near to saturation with respect to $Ca(OH)_2$ within a few minutes after mixing. This makes the paste extremely corrosive and precludes the use of many materials as specimen holders. The polished silicon wafers employed here appear to be a suitable material. The paste attacks the

silicon, forming a few etch pits in the surface. However, the result can only be the addition of a small amount of SiO_2 to the paste solution, which is not expected to affect the reaction rates.

Quasielastic neutron scattering (QNS) measurements at 60 μeV resolution were made using the 3-axis spectrometer TRIAX at the University of Missouri Research Reactor. These measurements have been made possible by recent advances in neutron optics (13). A pneumatically bent single crystal silicon wafer 15 cm in diameter was used as the monochromator for this work. An identical mechanically (cylindrically) bent silicon wafer served as the neutron energy analyzer. It can be shown that the instrumental energy resolution and scattered neutron intensity are dependant on the position and orientation of the specimen with respect to the neutron beam, neutron wavelength, spectrometer geometry, and the monochromator and analyzer bending radii. Optimization of the experimental configuration for these experiments will be the subject of another publication (10).

Various experimental checks on the performance of the instrument provide convincing evidence that the 60 μeV resolution can be routinely obtained and stably maintained over a period of several months. The majority of the measurements were made at $q = 1$ Å^{-1} although data from a series of measurements at various momentum transfers was also acquired. The q-dependence of the QNS can be used to model the nature of the environment of the diffusing water molecules and these results will be described in a subsequent paper (14).

Specimens were prepared at intervals over a period of 5 weeks and stored in a sealed container at room temperature and high ambient humidity. Other specimens were prepared and immediately placed on the spectrometer so that the kinetics of the hydration reaction could be followed through the early stage. All of the experiments were performed with the cement paste at room temperature.

Measurement of the QNS from a cement paste under the conditions of this experiment takes about 1.5 h and is accomplished by step-scanning the analyzer crystal at a fixed incident neutron energy of 10 meV. Because the general character of the scattering curves is known in advance, the scans optimize the definition of the Gaussian central peak by making smaller energy steps in the region around zero energy transfer. In all subsequent discussion, the time identified with a particular QNS spectrum corresponds to that of the middle of the scan.

Figure 2a shows a time sequence of QNS data from a hydrating C_3S paste with w/c = 0.5. In this figure, every other time slice is shown from just after mixing until nearly 40 h of hydration. The solid line through the data points is the fit to the data as described below. It is evident that the scattered neutron energy spectrum develops an increasing Gaussian elastic component as the paste reacts. In Figure 2b, analysis of the data from the time slice centered at 18.8 h is shown. Here, we have fit the data to a combination of three components: a Gaussian (elastically) scattered component with a width fixed at 60 μeV, as determined by the instrumental resolution, a Lorentzian component of variable width, and a flat background:

$$Counts = \frac{a_L}{(1 + (4(x - x_o))/w_L)^2} + a_G e^{(-((x - x_o)/w_G)^2)} + bkg \qquad (1)$$

In Eq. 1, x is the scattered neutron energy gain or loss, and w_G and a_G are the width and amplitude, respectively, of the Gaussian component. The quantities a_L and w_L are the amplitude and width of the Lorentzian component and the flat background is represented by *bkg*. The quantity x_o accounts for instrumental offsets that make the center of the scattered

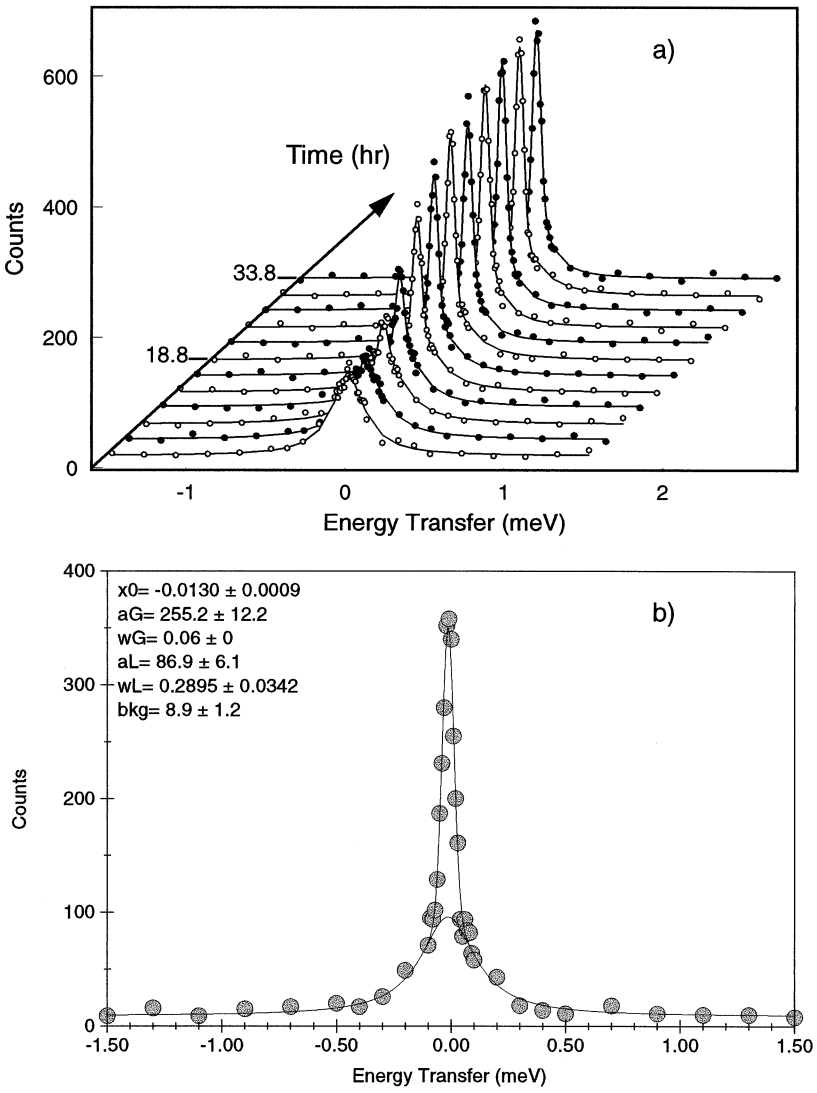

FIG. 2.

a) Time sequence of QNS data for a hydrating C_3S w/c = 0.5 specimen. Every other time slice is shown. *b*) Fit of typical QNS data at 18.8 h to three components: a flat background, a Gaussian of width 60 μeV, and a Lorentzian. The two solid lines show the trace of the Lorentzian component and the agreement of the data and fit to all three components. The values of the fit parameters are shown in the upper left corner of the figure.

neutron energy spectrum appear to be slightly different from zero. The solid lines in Figure 2b show the fit to the data using Eq. 1 as well as the contribution of only the Lorentzian and background components of that fit. The ratio of the signal from bound water (the integral of the Gaussian) to the total signal (sum of the Gaussian and Lorentzian) is the bound water index (BWI), which is zero at the start of hydration and increases as the hydration reactions

proceed. Tables of the BWI vs. time for the specimens studied in this experiment appear in the Appendix.

These measurements are of limited time and BWI resolution. We anticipate, however, substantial improvements in the available neutron flux on-sample in the coming months (15). These improvements will allow us to make QNS measurements with significantly better time resolution and with smaller statistical uncertainties in the determination of the BWI. With this new instrumentation, more extensive investigations of cement hydration, including the effects of temperature, will be undertaken.

Discussion

In a C_3S paste with a high w/c ratio, more than enough water is present to hydrate all the C_3S, and the BWI will never reach 1. Similarly, in a paste with low w/c ratio, some C_3S will necessarily remain unhydrated even though the BWI approaches unity. The experimentally measured BWI can be related to the degree of reaction (the fractional amount of cement consumed) using the stoichiometry of the hydration reactions. Fuji and Kondo (16) write the hydration reaction as:

$$(3CaO{\cdot}SiO_2) + 3.9H_2O = 1.68CaO{\cdot}SiO_2{\cdot}2.58H_2O + 1.32Ca(OH)_2 \qquad (2)$$

When S moles of C_3S are mixed with Y moles of H_2O, it is straightforward to show that:

$$\mathrm{BWI} = \frac{3.9\alpha S}{Y} = \frac{3.9\alpha}{12.7(\mathrm{w/c})} \qquad (3)$$

where w/c is the water-to-cement ratio by weight, α the degree of reaction, and the quantity 12.7 the ratio of the molecular weights of C_3S and H_2O. Equation 3 allows us to present the data in terms of the degree of reaction in Figure 3.

The Avrami model can be used to model nucleation and growth reaction kinetics in order to determine the general morphology of reaction products and the rate-limiting step of the reaction (17–19). The basic Avrami equation is:

$$\alpha = 1 + \alpha_o - e^{k(t - t_o)^M} \qquad (4)$$

where α_o is the degree of reaction at the time t_o when this nucleation and growth process becomes dominant and k is a rate constant that combines the effects of nucleation, multidimensional growth, geometric shape factors, and diffusion. The exponent M is related to the nature of the reaction through the parameters P, Q, and S:

$$M = \frac{P}{S} + Q \qquad (5)$$

where P is related to the dimensionality of the product phase: $P = 3$, $P = 2$, and $P = 1$ corresponding to the growth of polygonal forms, sheets, and fibers (needles), respectively. Similarly, S describes the type of growth, with $S = 1$ corresponding to interfacial or phase boundary growth and $S = 2$ corresponding to diffusion of components though the liquid phase. Finally, Q is related to the nucleation rate: $Q = 0$ for no nucleation and $Q = 1$ for constant nucleation. This analysis has previously been applied to C_3S hydration (20) using kinetic data obtained by calorimetry, QXDA, and thermo-gravimetry (21,22), resulting in M

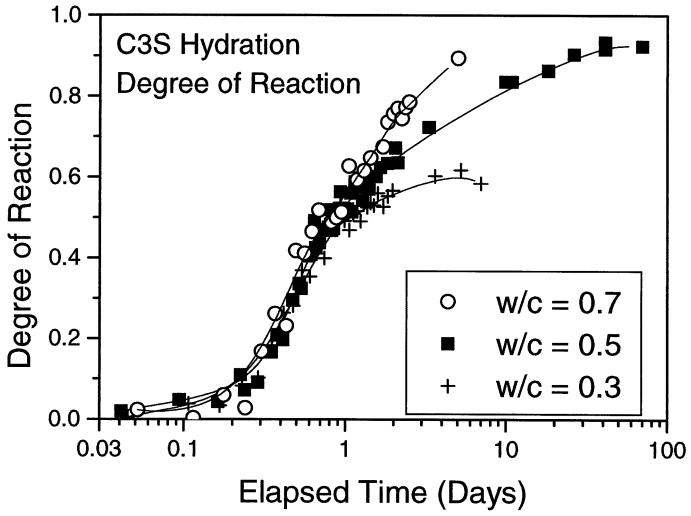

FIG. 3.
The degree of reaction (fraction of cement consumed) vs. time for C_3S at three different water/cement (w/c) ratios. The results from 6 different specimens: C3S0–C3S5 were combined to obtain the result for w/c = 0.5. Cubic spline fits have been used to form the lines through the data.

between 0.67 and 1. In addition, a recent Raman scattering study of C_3S hydration obtained an exponent $M = 0.85$ (3).

A least-squares fit to the data employing the logarithmic form of Eq. 4 can be used to obtain k and M once the appropriate values of α_o and t_o have been chosen. Data for the early hydration period (from mixing until ~40 h) were analyzed for the three w/c = 0.5 specimens labeled C3S0, C3S4, and C3S5. A plot of the degree of reaction as a fit to the logarithmic form of Eq. 4 is shown in Figure 4. The straight line fit to this data was obtained with $\alpha_o = 0$ and $t_o = 0$ over the period $0 < t < 15$ h. Attempts to obtain values of α_o and t_o different from zero did not lead to an improvement in the quality of the fit to the data.

The results of the fit to Eq. 4 for the three different w/c ratios measured in this experiment are shown in Table 1.

At very early times of hydration, it is difficult to accurately determine the BWI and it may be reasonable to expect that these values represent the "sensitivity floor" of the experiment. If data with $\log t < 1$ is excluded, the fit of Eq. 4 to the data yields 2.06 ± 0.11, 1.93 ± 0.08, and 1.84 ± 0.11 for the exponent M at w/c = 0.3, 0.5, and 0.7, respectively.

TABLE 1
Avrami parameters for C_3S hydration.

w/c	M	$\log(k)$
0.3	1.86 ± 0.09	−5.55 ± 0.20
0.5	1.72 ± 0.06	−5.19 ± 0.16
0.7	1.66 ± 0.19	−4.92 ± 0.45

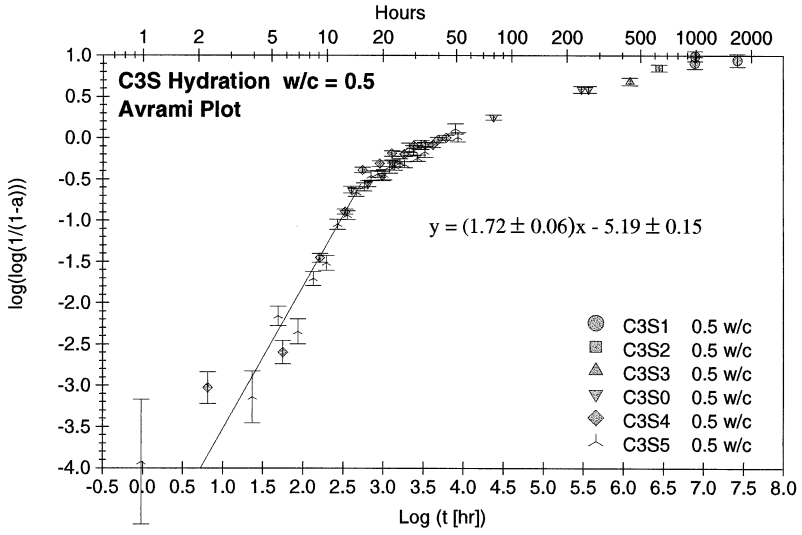

FIG. 4.
A plot of the logarithmic form of Eq. 4 for the hydration data of C_3S specimens with w/c = 0.5. If the first two data points are excluded from the fit, a slope of 1.93 ± 0.08 is obtained.

The most interesting aspect of these results is the value of the exponent M obtained. A value of $M = 2$ is consistent with (P, S, Q) = (2, 1, 0) and (P, S, Q) = (2, 2, 1) that is plate-type product phase and phase boundary growth with constant nucleation or diffusion controlled growth with no nucleation. It is also consistent with (P, S, Q) = (1, 1, 1); needle-type product phase morphology, phase boundary growth, and constant nucleation. These results are at variance with the earlier kinetic analyses (20).

Although identification of the BWI with chemically combined water is clear, the connection between the BWI and the degree of reaction is dependent on the stoichiometry of the hydration reactions. If the amount of water incorporated into the C-S-H phase changes appreciably as the reaction proceeds, then the assumed relationship between the BWI and the degree of reaction defined in Eq. 4 will not hold.

At long times, ($t > 20$ h) the cement grains are covered by a growing layer of C-S-H product and the kinetics are controlled by the rate of diffusion through this layer. At this point, the rate of hydration depends strongly on the w/c ratio (See Fig. 3). Following Fuji and Kondo (16), we can write the rate of reaction as:

$$(1 - \alpha)^{1/3} = -(2K)^{1/2}(t - t^*)^{1/2}/R + (1 - \alpha^*)^{1/3} \quad (6)$$

where K is the diffusion constant (cm^2/h), α and α^* are the degrees of reaction at the times t and t^*, and R is the original radius of the cement grains. A plot of $(1 - \alpha)^{1/3}$ vs. $(t - t^*)^{1/2}$ demonstrates agreement with Eq. 6 and provides a value for K if the radius of the cement particles is sufficiently monodisperse. Figure 5 is an example of this analysis for the data from C_3S (specimens C3S0, . . . , C3S5) with w/c = 0.5. A line was fit to the data over the range of 20 h $< t <$ 900 h with $t^* = 30$ h. The quality of the fit to Eq. 6 is better than that with $t^* = 20$ h as would be expected—at longer times, diffusion is the dominant influence on the reaction rate. While data on C_3S w/c = 0.5 specimens was available at times up to 60

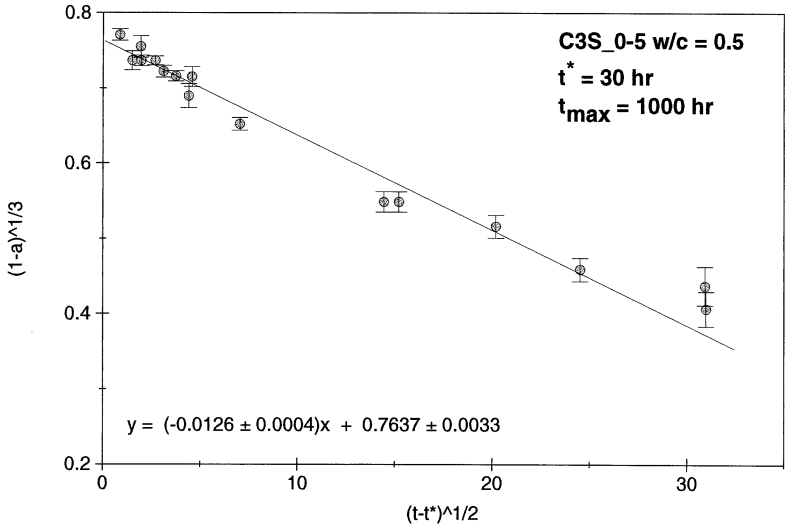

FIG. 5.
Determination of the diffusion constant for the diffusion limited period of C_3S hydration. The straight line fit to the data gives $(2K)^{1/2}/R$ as the slope of the line.

days, the data for the w/c = 0.3 and w/c = 0.7 specimens only extended to 7 days and 5 days, respectively.

Values of the diffusion constant, *K*, obtained from the fits to data and using the measured mean of the particle size distribution for *R* in Eq. 6 are summarized in Table 2.

These data are plotted in Figure 6 revealing a log-linear relationship between the diffusion constant obtained for the diffusion limited portion of the hydration reaction and the w/c ratio. Slightly different values of *K* are obtained dependent on the value of *t** and the "long-time" extent of the data. With *t** = 30 h the apparent diffusion constant obtained from this analysis is larger than that for *t** = 20 h as would be expected. The C-S-H covering the unhydrated grain cores is believed to become denser and less permeable as the reaction proceeds.

A number of workers have proposed modifications of the kinetic analysis to include the effect of the particle size distribution of the cement grains (24–28). Knudson (25) argues that ". . . only gross features in the kinetics governing the hydration of a singe particle may be discovered by the hydration curve" because of the dominance of the effect of particle size distribution on the rate of hydration. We have chosen not to include the effect of particle size distribution in analysis of this experiment. The distribution is sufficiently narrow that its effect is reduced during the nucleation and growth period—only a small fraction of the

TABLE 2
Diffusion constants for C_3S hydration at different w/c ratios.

Specimen	w/c	*t** hr	tmax hr	*K* (10^{-10} cm^2/hr)
C3S6	0.3	30	166	0.42 ± 0.12
C3S0-5	0.5	30	1000	2.64 ± 0.16
C3S7	0.7	30	121	15.6 ± 2.7

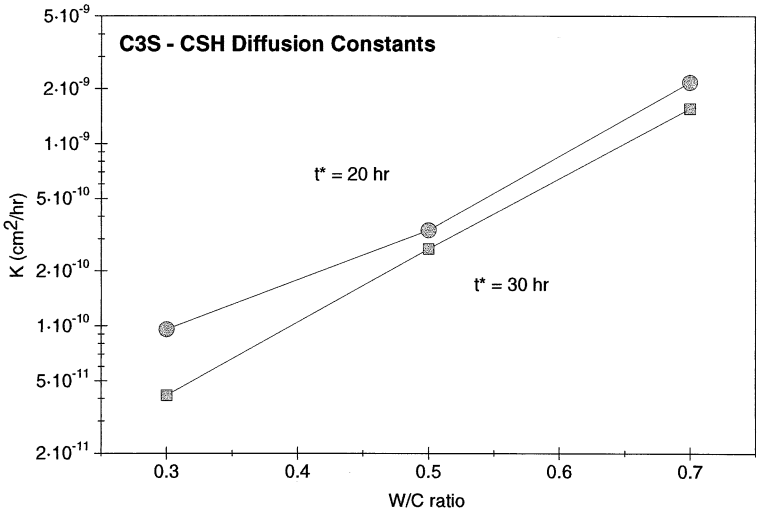

FIG. 6.
The variation of the diffusion constant of C-S-H produced from C_3S as a function of the w/c ratio. The results with $t^* = 20$ h are larger than those for $t^* = 30$ h because the C-S-H layer is expected to become thicker and denser as the reaction proceeds.

cement grains will be fully hydrated at the end of this time (~15 h) (27). Neglect of the particle size distribution is more important in analysis of the diffusion-limited region of the hydration curves. Clearly the particle size enters directly into the determination of the diffusion constant. Nevertheless, the interesting result here is the log-linear relationship between the diffusion constant and the w/c ratio, which we expect to be relatively independent of the size distribution.

Summary and Conclusions

Quasielastic neutron scattering was used to monitor the early hydration of C_3S. With this technique, the amount of bound and free water can be monitored with time, and the ratio of the amount of chemically bound water to the total amount of water, the BWI, was used to determine the degree of reaction over the first few days. The hydration of C_3S at three different w/c ratios, 0.7, 0.5, and 0.3, was studied in this experiment. It was possible to fit the data from the nucleation and growth period of the reaction to an Avrami model and to obtain the exponent M that is indicative of the nature of the reaction. We find that this exponent is approximately 1.75 if all the data is included in the determination. If the earliest time data is excluded, this exponent is 2 within experimental error. In either case, this is interpreted as the result of phase boundary growth and constant nucleation with either a plate-type or needle (fiber) product-phase morphology or of diffusion limited growth with no nucleation and a plate-type product morphology. While the initial rate of reaction is nearly independent of the water-to-cement ratio, after approximately 15 h the hydration rate becomes diffusion controlled and strongly dependent on the w/c ratio. A higher degree of reaction is obtained with the higher w/c ratio. The kinetics of the hydration reaction at long times after mixing was analyzed with a "shrinking core" model to obtain values of the rate-limiting diffusion

constant. Using the mean of the particle size distribution as the C_3S grain size, diffusion constants were obtained. The diffusion constants exhibit a log-linear (exponential) relationship as a function of w/c ratio in the range $0.3 <= w/c <= 0.7$.

Acknowledgments

This work was partially supported by the U.S. Department of Energy under contract DE-FG02–96ER45599. The authors extend their thanks to Mr. Aaron Saak of Northwestern University for making the particle size distribution measurements.

References

1. H.W.F. Taylor, Cement Chemistry, Academic Press, London, 1990.
2. R. Berliner, F. Trouw, and H. Jennings, Bull. Am. Phys. Soc. 40, 665 (1995).
3. M. Tarrida, M. Madon, B. Le Rolland, and P. Colombet, Adv. Cem. Bas. Mater. 2, 15–20 (1995).
4. S.M. Clark and P. Barnes, Cem. Concr. Res. 25, 639 (1995).
5. NIST Reactor, Summary of Activities, October 1992 through September 1993, p 7.
6. NIST Reactor, Summary of Activities, October 1993 through September 1994, p 5.
7. R.A. Livingston, D.A. Neumann, A. Allen, and J.J. Rush, Application of Neutron Scattering Methods to Cementitious Materials, D. Neumann, T.P. Russell, and B.J. Wuensch (eds.), Mater. Res. Symp. Proc. 376, 1995.
8. G.E. Bacon, Neutron Diffraction, Clarendon Press, Oxford, 1975.
9. T. Springer, Quasielastic Neutron Scattering for the Investigation of Diffuse Motions in Solids and Liquids. Springer Tracts in Modern Physics, p. 64, Springer-Verlag, Berlin, 1972.
10. M. Popovici, K.W. Herwig, R. Berliner, W.B. Yelon, and L. Groza, High-resolution neutron scattering with commercial thin silicon wafers as focusing monochromators, in preparation.
11. R. Berliner, M. Popovici, K.W. Herwig, M. Berliner, H. Jennings, and J. Thomas, Bull. Am. Phys. Soc. 41, 76 (1997).
12. The cement particle size distribution was measured by a Coulter LS130 Particle Size Analyzer. Coulter Corporation, P.O. Box 2145, Hialeah, Florida 33012–9975.
13. M. Popovici, W.B. Yelon, R. Berliner, and A.D. Stoica, Proceedings of the Workshop on Neutron Scattering Instrument Design, pp. 23–25, Berkeley, CA, September, 1996.
14. R. Berliner, K.W. Herwig, and M. Popovici, Quasielastic neutron scattering from the water in C-S-H, in preparation.
15. We anticipate installing a new neutron monochromator with a $\times 20$ increase in sample flux at 10 meV incident energy.
16. K. Fujii and W. Kondo, J. Am. Ceram. Soc. 57, 492 (1974).
17. M. Avrami, J. Chem. Phys. 7, 1103 (1939).
18. M. Avrami, J. Chem. Phys. 8, 212 (1939).
19. M. Avrami, J. Chem. Phys. 9, 177 (1940).
20. P. W. Brown, J. Pommersheim, and G. Frohnsdorff, Cem. Concr. Res. 15, 33–41 (1985).
21. R. Kondo and S. Ueda, V Intl. Sym. Chem. Cement, II, 203, Tokyo, 1968.
22. I. Odler and J. Schuppstuhl, Cem. Concr. Res. 11, 765 (1981).
23. The data of Tarrida et al. does not extend to the low degree of reaction that was obtained in this work. Discarding the first few data points following mixing in our experiment, the earliest value of $[\log(t), \log(\log(1/1 - \alpha))]$ in their work is $[1.37, -1.4]$ in comparison to $[-0.016, -3.9]$ measured in this experiment.
24. A. Bezjak and I. Jelenic, Cem. Concr. Res. 10, 553–563 (1980).
25. T. Knudsen, Cem. Concr. Res. 14, 622–630 (1984).
26. A. Bezjak, Cem. Concr. Res. 16, 260–264 (1986).

27. M. Slater, S. Song, A. Saglik, B.J. Christensen, and H. M. Jennings, Relationship Between Rate of Hydration and Physical and Chemical Characteristics of Portland Cement, p. 9, unpublished.
28. P.W. Brown, J. Am. Ceram. Soc. 72, 1829–32 (1989).

Appendix

Bound Water Index for C_3S Hydration

APPENDIX 1
BWI for C_3S Specimens with w/c = 0.5.

C3S0 time (days)	BWI
0.563	0.254 ± 0.016
0.694	0.268 ± 0.014
0.825	0.287 ± 0.023
0.940	0.320 ± 0.016
3.311	0.444 ± 0.013
9.942	0.513 ± 0.015
10.89	0.513 ± 0.015
C3S1 time (days)	BWI
41.11	0.563 ± 0.018
41.26	0.573 ± 0.014
52.75	0.618 ± 0.016
69.96	0.567 ± 0.019
C3S2 time (days)	BWI
26.30	0.555 ± 0.012
C3S3 time (days)	BWI
26.30	0.555 ± 0.012
C3S4 time (days)	BWI
0.094	0.029 ± 0.011
0.240	0.044 ± 0.012
0.380	0.128 ± 0.012
0.521	0.206 ± 0.010
0.647	0.302 ± 0.014
0.802	0.319 ± 0.014
0.933	0.346 ± 0.014
1.086	0.344 ± 0.013
1.228	0.367 ± 0.014
1.411	0.369 ± 0.014
1.552	0.369 ± 0.012
1.654	0.383 ± 0.015
1.835	0.389 ± 0.013
C3S5 time (days)	BWI
0.041	0.012 ± 0.018
#0.102	0.0 ± 0.013

APPENDIX 1
Continued

0.164	0.026 ± 0.016
0.226	0.067 ± 0.015
0.289	0.056 ± 0.016
0.350	0.102 ± 0.016
0.412	0.121 ± 0.019
0.474	0.182 ± 0.019
0.536	0.199 ± 0.017
0.598	0.248 ± 0.019
0.659	0.261 ± 0.019
0.720	0.288 ± 0.024
0.782	0.292 ± 0.017
0.845	0.290 ± 0.025
0.907	0.310 ± 0.031
0.968	0.311 ± 0.018
1.031	0.320 ± 0.024
1.092	0.316 ± 0.016
1.155	0.361 ± 0.025
1.218	0.353 ± 0.027
1.281	0.333 ± 0.017
1.344	0.369 ± 0.025
1.407	0.350 ± 0.030
2.059	0.413 ± 0.028
2.121	0.390 ± 0.025

APPENDIX 2
BWI for C_3S Specimens with w/c = 0.3.

C3S6 time (days)	BWI
0.045	0.005 ± 0.019
0.107	0.038 ± 0.015
0.168	0.033 ± 0.016
0.230	0.083 ± 0.019
0.291	0.103 ± 0.021
0.353	0.183 ± 0.016
0.415	0.264 ± 0.027
0.478	0.281 ± 0.039
0.540	0.369 ± 0.031
0.603	0.354 ± 0.026
0.665	0.411 ± 0.033
0.742	0.399 ± 0.018
0.805	0.480 ± 0.031
0.867	0.488 ± 0.038
0.930	0.537 ± 0.039
0.992	0.492 ± 0.028
1.060	0.469 ± 0.019
1.122	0.509 ± 0.023
1.185	0.516 ± 0.024
1.248	0.491 ± 0.041
1.311	0.536 ± 0.027
1.374	0.525 ± 0.036
1.437	0.536 ± 0.028
1.499	0.530 ± 0.037
1.595	0.560 ± 0.028
1.719	0.527 ± 0.017
1.844	0.553 ± 0.017
1.969	0.567 ± 0.022
3.610	0.603 ± 0.017
5.210	0.618 ± 0.031
6.953	0.584 ± 0.028

APPENDIX 3
BWI for C_3S Specimens with w/c = 0.7.

C3S7 time (days)	BWI
0.052	0.010 ± 0.014
0.115	0.001 ± 0.018
0.178	0.026 ± 0.022
0.242	0.012 ± 0.042
0.305	0.074 ± 0.028
0.369	0.115 ± 0.020
0.433	0.102 ± 0.017
0.497	0.184 ± 0.025
0.561	0.181 ± 0.027
0.625	0.205 ± 0.019
0.689	0.228 ± 0.021
0.822	0.215 ± 0.021
0.886	0.220 ± 0.026
0.951	0.226 ± 0.034
1.057	0.276 ± 0.016
1.184	0.261 ± 0.018
1.311	0.271 ± 0.015
1.438	0.285 ± 0.014
1.717	0.297 ± 0.018
1.843	0.324 ± 0.018
1.997	0.333 ± 0.019
2.123	0.339 ± 0.020
2.248	0.328 ± 0.018
2.375	0.340 ± 0.017
2.502	0.346 ± 0.017
5.042	0.394 ± 0.016